

See discussions, stats, and author profiles for this publication at: <https://www.researchgate.net/publication/343840828>

# From mountains to cities: a novel isotope hydrological assessment of a tropical water distribution system

Article in *Isotopes in Environmental and Health Studies* · August 2020

DOI: 10.1080/10256016.2020.1809390

CITATIONS

0

READS

16

8 authors, including:



**Ricardo Sánchez-Murillo**  
National University of Costa Rica

155 PUBLICATIONS 497 CITATIONS

[SEE PROFILE](#)



**Germain Esquivel Hernández**  
National University of Costa Rica

102 PUBLICATIONS 277 CITATIONS

[SEE PROFILE](#)



**Christian Birkel**  
University of Costa Rica

157 PUBLICATIONS 2,058 CITATIONS

[SEE PROFILE](#)



**Lucía Ortega**  
International Atomic Energy Agency (IAEA)

17 PUBLICATIONS 39 CITATIONS

[SEE PROFILE](#)

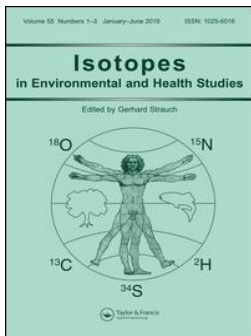
Some of the authors of this publication are also working on these related projects:



Isodrones - Resolving the mystery of deep roots: combining water stable isotopes with next generation technology [View project](#)



Los impactos hidrológicos y de desarrollo de El Niño en Costa Rica [View project](#)




## From mountains to cities: a novel isotope hydrological assessment of a tropical water distribution system

Ricardo Sánchez-Murillo , Germain Esquivel-Hernández , Christian Birkel , Lucia Ortega , Michael Sánchez-Guerrero , Luis Daniel Rojas-Jiménez , José Vargas-Viquez & Laura Castro-Chacón

To cite this article: Ricardo Sánchez-Murillo , Germain Esquivel-Hernández , Christian Birkel , Lucia Ortega , Michael Sánchez-Guerrero , Luis Daniel Rojas-Jiménez , José Vargas-Viquez & Laura Castro-Chacón (2020): From mountains to cities: a novel isotope hydrological assessment of a tropical water distribution system, *Isotopes in Environmental and Health Studies*, DOI: [10.1080/10256016.2020.1809390](https://doi.org/10.1080/10256016.2020.1809390)

To link to this article: <https://doi.org/10.1080/10256016.2020.1809390>

 [View supplementary material](#) 

 Published online: 24 Aug 2020.

 [Submit your article to this journal](#) 

 [View related articles](#) 

 [View Crossmark data](#) 



## From mountains to cities: a novel isotope hydrological assessment of a tropical water distribution system

Ricardo Sánchez-Murillo<sup>a</sup>, Germain Esquivel-Hernández<sup>a</sup>, Christian Birkel<sup>b</sup>,  
Lucia Ortega<sup>b,c</sup>, Michael Sánchez-Guerrero<sup>d</sup>, Luis Daniel Rojas-Jiménez<sup>d</sup>, José Vargas-  
Viquez<sup>d</sup> and Laura Castro-Chacón<sup>d</sup>

<sup>a</sup>Stable Isotopes Research Group and Water Resources Management Laboratory, School of Chemistry, Universidad Nacional, Heredia, Costa Rica; <sup>b</sup>Department of Geography and Water and Global Change Observatory, University of Costa Rica, San José, Costa Rica; <sup>c</sup>International Atomic Energy Agency, Isotope Hydrology Section, Vienna International Center, Vienna, Austria; <sup>d</sup>Empresa de Servicios Públicos de Heredia (ESPH), Heredia, Costa Rica

### ABSTRACT

Water use by anthropogenic activities in the face of climate change invokes a better understanding of headwater sources and lowland urban water allocations. Here, we constrained a Bayesian mixing model with stable isotope data (2018–2019) in rainfall ( $N = 704$ ), spring water ( $N = 96$ ), and surface water ( $N = 94$ ) with seasonal isotope sampling (wet and dry seasons) of an urban aqueduct ( $N = 215$ ) in the Central Valley of Costa Rica. Low  $\delta^{18}\text{O}$  rainfall compositions corresponded to the western boundary of the study area, whereas high values were reported to the northeastern limit, reflecting the influence of moisture transport from the Caribbean domain coupled with strong orographic effects over the Pacific slope. The latter is well-depicted in the relative rainfall contributions (west versus east) in two headwater systems: (a) spring ( $68.7 \pm 3.4\%$ , west domain) and (b) stream ( $55.8 \pm 3.9\%$ , east domain). The aqueduct exhibited a spatial predominance of spring water and surface water during a normal wet season (78.7%), whereas deep groundwater and spring water were fundamental sources for the aqueduct in the dry season (69.4%). Our tracer-based methodology can help improve aqueduct management practices in changing climate, including optimal water allocation and reduced evaporative losses in the dry season.

### ARTICLE HISTORY

Received 3 April 2020

Accepted 6 July 2020


### KEYWORDS

Aqueduct management; Bayesian mixing model; Costa Rica; hydrogen-2; isotope hydrology; oxygen-18; urban hydrology

## 1. Introduction

Water is recognized as the most fundamental and indispensable of all natural resources. One of the sustainable development goals (SDGs No.6) [1] adopted by world leaders was to ensure the human right of access to water and sanitation for all by 2030, recognizing that clearly neither socio-economic development nor environmental diversity can be sustained without water. However, unequal distribution at different scales and unsustainable water use are creating tensions over water allocation worldwide [2–5]. In Costa Rica, a

**CONTACT** Ricardo Sánchez-Murillo ✉ ricardo.sanchez.murillo@una.cr

 Supplemental data for this article can be accessed at <https://doi.org/10.1080/10256016.2020.1809390>.

© 2020 Informa UK Limited, trading as Taylor & Francis Group

nation with a vast water capital of  $\sim 2.8 \times 10^4 \text{ m}^3/\text{person-year}$  [6], over 700 water conflicts [7] emerged during the last decade as a response to limited water availability during recurrent El Niño-Southern Oscillation (ENSO) drought events and inefficient water use. This study demonstrated that roughly 80 % of the conflicts occurred due to inadequate water infrastructure or a lack of scientific knowledge ranging from groundwater recharge processes to water distribution in the main lowland urban areas.

The inherent complexity of urban water distribution or aqueduct systems (i.e. storage units, pumping stations, transfer lines, pipe longevity and location, channels and canals, multiple leakages/fractures, illegal water withdraws, and programmed or unexpected shortages) invokes the need of traceable water techniques to underpin connections and temporal and spatial discontinuities within aqueduct networks. Lately, novel applications of water stable isotopes have served to improve our current understanding of urban aqueducts in temperate regions (mostly across western USA, China, and Europe) including the identification of tap water sources and mixing ratios, groundwater-surface water connectivity, aqueduct dynamics, urban infiltration losses, and storage and transport in the context of rapid urban growth and inter-annual climate variability [8–16]. In contrast, to our knowledge, detailed urban hydrology studies of aqueduct processes are scarce or incipient across the humid tropics.

In high relief tropical regions, lowland cities largely depend on water recharge across mountain ranges. For example, in the Central Valley of Costa Rica, a drinking water company (known as ESPH) serves potable water to over 242,000 inhabitants using a variety of water sources including surface water, spring water, and shallow and deep wells (up to  $\sim 300 \text{ m}$  depth). The overall contribution of each source changes throughout the water year (or inter-annually) depending on rainfall seasonality and spatial water availability. Commonly, during rainfall surplus periods water movement by gravity is favored (e.g. elevation gradient of roughly  $1500 \text{ m asl}$ ); however, during rainfall deficits (due to the strong recession in spring and surface water sources) groundwater pumping becomes the main water source at the expense of a greater electricity consumption and cost. For instance, between 2013 and 2019 the average rainfall deficit reached 19.4 % with a maximum deficit (2015: 40.4 %) during the last very strong El Niño event [17], when compared to the long-term mean annual rainfall (normal period: 1982–2012:  $2452 \pm 88 \text{ mm}$ ) [18]. This recurrent situation poses a challenging scenario for water security, and consequently, an effective and equal water distribution across the aqueduct network during the dry season.

Environmental isotopes have become a well-established and reliable tool in many fields of hydrology, as isotopes can provide important information to water managers for assessing sources and interactions between water bodies. Isotopically, rainfall variability across the northern region of the Central Valley of Costa Rica offers a practical advantage. Rainfall seasonality between the Pacific (whereby most of the Central Valley is located) and Caribbean slopes (being the Caribbean Sea the main moisture source), results in a clear and significant spatio-temporal isotope separation [19–22]. These distinct isotopic pulses are transferred with different residence times to surface water networks and shallow/deep aquifers, and later, to a wide variety of aqueducts or distribution systems from mountain locations to lowland urban areas. However, the spatial variability of water movement during different climatic pressures (i.e. water excess or scarcity) remains largely unknown in tropical urban areas.

To fill this knowledge gap and to provide a novel methodology to underpin processes in tropical urban areas, we focused on short-term (2–3 days), intense experimental campaigns to collect tracer data with a relatively high spatial resolution in a variety of aqueduct features between 2018 and 2019 (two wet and one dry seasons). The monitoring included main sources such as rainfall, streams, springs, and wells as well as engineering features such as storage tanks, transfer lines/pumping units, and tap water across the distribution system. Therefore, this pioneer isotope urban hydrology study combines spatio-temporal variations of stable isotopes and hydraulic information [9,13] to address the following specific objectives:

- (1) Estimate multiple isotope source water contributions to assess water allocation in a tropical water distribution system during contrasting wet and dry conditions.
- (2) Compare groundwater versus surface water mixing ratios during wet and dry seasons to evaluate engineering management practices such as source water switching during periods of water stress.

Our study could serve as a pilot effort for understanding water routes within the aqueduct throughout the hydrological cycle as well as a traceable tool of engineering practices in a complex array of water sources and pipeline assemblages (some of them unknown due to their longevity) in a humid region but recurrently affected by ENSO-related droughts in recent years.

## 2. Study area

### 2.1. Geological and climate characteristics

The aqueduct study area corresponds to the boundaries of the Barva–Colima multi-aquifer system (BCS), in the northern section of the Virilla River watershed (Figures 1 and 2). Geological formations comprise highly fractured and brecciated material from the volcanoes of the Central Volcanic Range in the headwaters (>1500–2906 m asl), mainly due to the activity of the Barva volcano during the Quaternary period [23]. The BCS is divided into two important aquifers: Barva and Colima. The Barva formation is a shallow unconfined aquifer, and the Colima aquifer is subdivided into two aquifers: Upper Colima (semi-confined) and Lower Colima (confined) [24]. The basements of both aquifers are constituted of low-permeability tuffs that allow water accumulation in the upper layers, being of great importance for water supply to the Greater Metropolitan Area [25] of Costa Rica (Figure 2, upper panel).

Climate is controlled by the trade winds from the northeast, the seasonal shift of the Intertropical Convergence Zone (ITCZ), cold fronts, and the indirect influence of tropical cyclones [26]. Latitudinal (north–south) ITCZ migrations affect rainfall seasonality in Costa Rica. During the dry season, the ITCZ is located south of this region, while during the wet season, the ITCZ poses over Central America, bringing atmospheric instability and large rainfall amounts. In the Pacific slope (urban area), rainfall occurs from May to mid-November. On the other hand, the Caribbean regime (high elevation recharge area; >1550 m asl) is influenced by trade winds from the northeast, and it does not have a well-defined dry season since the rainfall rate in the drier months is between 100 and

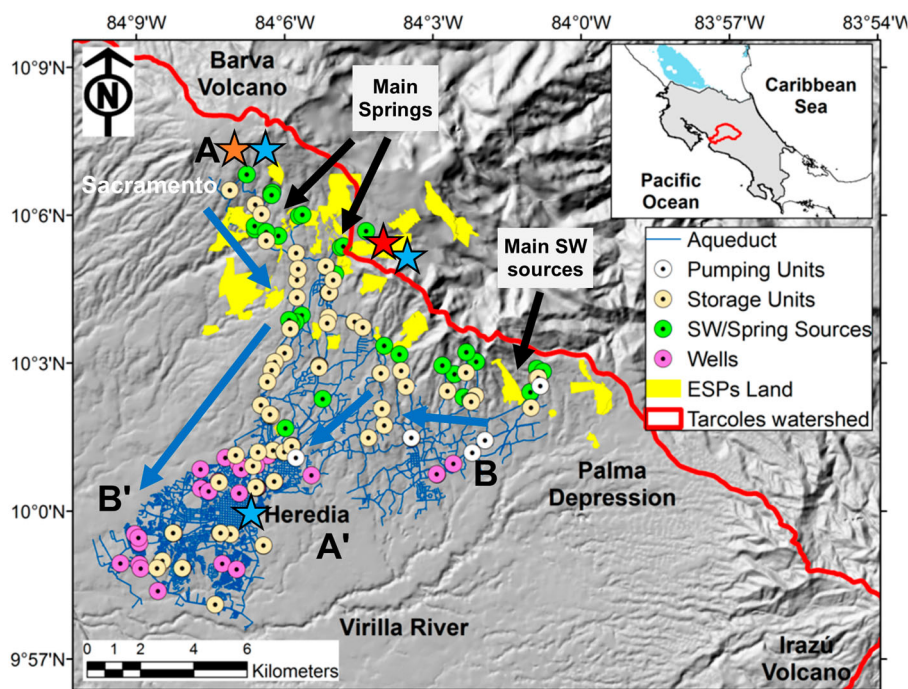


**Figure 1.** Water distribution system including spring/surface water sources, wells, transfer lines, and storage units/tanks. The bold line denotes the limits of the Virilla/Tárcoles watershed within the continental divide (Pacific versus Caribbean slopes). Polygons represent private properties under the Environmental Services Payment scheme [23] within the most important recharge area. Thin lines represent the pipeline network with an estimated length of 945 km. Heredia is the main city within the aqueduct structure. Stars denote rainfall collection sites in the urban area (Heredia), headwaters (west and east sites), and spring and surface monitoring sites. Inset shows the relative location of the study area in central Costa Rica. Lithological cross sections between A–A' and B–B' are presented in the upper panel of Figure 2. Bold arrows indicate main water paths from headwater sources to the lowland urban area. The area is located between two volcano edifices (Barva and Irazú) separated by a wind pass (NE prevailing winds) known as Palma Depression.

200 mm [27] (Figure 2, lower panel). In general, the high elevation regions of central Costa Rica are characterized by a cold (12.5 °C) and rainy (>3000 mm) climate. In the middle section, the climate is mild (17.5 °C), and in the lowlands, the climate is warm (23.0 °C) and less wet (2000 mm).

## 2.2. Water distribution system characteristics

The aqueduct comprises three main water sources: springs ( $N=17$ ), wells ( $N=25$ ), and surface waters ( $N=11$ ). Most of the springs and surface water sources are located above 1576 m asl, whereas wells ranged from 996 to 1333 m asl except for one well located at 1829 m asl (Figure 1). Wells depths ranged from 61 to 352 m with pumping rates fluctuating from 7 to 85 L/s. Static and dynamic water levels fluctuated from 45 to 258 m and 51–261 m, respectively. Overall, by January 2020 springs/streams and wells

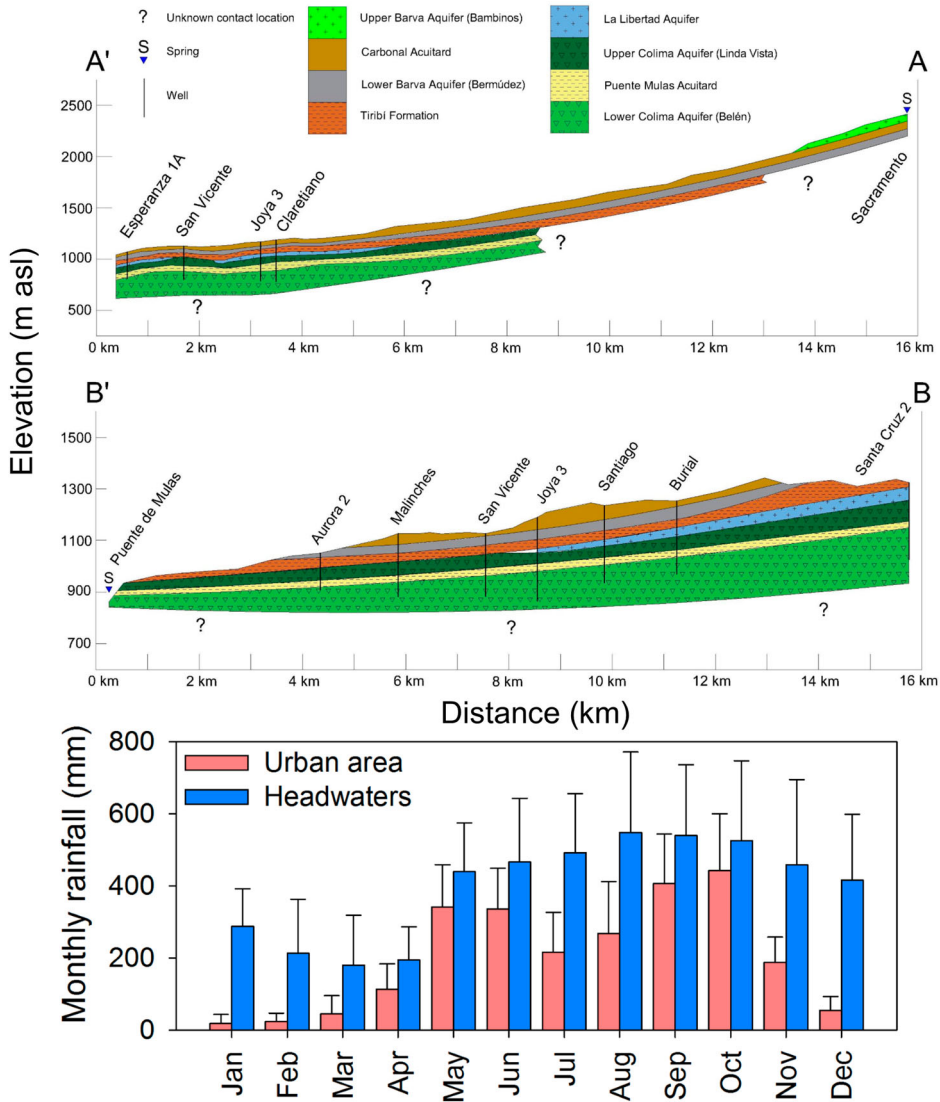


**Figure 2.** Upper panel: Lithological cross sections of transects A–A' (N–S) and B–B' (E–W) within the study area (see Figure 1). This multi-aquifer system comprises one unconfined aquifer (Barva) and two deeper semi-confined aquifers (Colima) [24]. Lower panel: Long-term monthly rainfall (mm) within the headwaters of Barva volcano and the urban area of Heredia. Error bars denote ( $1\sigma$ ) long-term monthly standard deviations.

provided 190 and 872 L/s, adding to a total offer of 1062 L/s, respectively. Residential and business services (i.e. industry and commerce) demanded between 910 and 130 L/s, a total of 1040 L/s. Approximately 1000 hectares of private properties form part of the Environmental Services Payment (i.e. payment for forest conservation and ecosystem services) [28] within the main recharge area (above 1550 m asl; Figure 1).

This system provides water to 73,679 subscribers, resulting in a total population close to 242,000 inhabitants. The average number of residents per house is  $\sim 3.28$ . The longevity of



the aqueduct is variable. Historical records indicate installation for some storage and pressure control tanks back to 1892–1902. However, most of the current pipeline networks were installed between 1957 and 1960. In the last decades, however, several projects have replaced old pipelines across the aqueduct. In general, total pipeline length is about 915 km and comprises 84 storage tanks, 6629 gate valves, 156 hydraulic special valves, and 1609 hydrants.

### 3. Materials and methods

The rationale behind our experimental design relies on the need to integrate the understanding of hydrological processes at the headwaters and recharge areas as active components of the water distribution system in a tropical urban scenario. Therefore, sampling campaigns targeted representative water sources at high elevations such as springs and streams as well as the main water source at the urban setting, mostly deep groundwater wells. Endmember contributions were further evaluated across the water distribution system using a Bayesian mixing model as described in the following sections.

#### 3.1. Aqueduct sampling

Three isotope sampling campaigns were designed to capture: (a) the climatic seasonality (wet and dry seasons), (b) the spatial variability across the pipeline network and water sources, and (c) the representativeness of all aqueduct features described in section 2.1. Regular aqueduct operation during rainfall peaks and water stress episodes constrained the number of samples in each sampling campaign. Two wet seasons were sampled in September 2018 ( $N = 110$ ) and September 2019 ( $N = 105$ ), whereas one very dry season was sampled in April 2020 ( $N = 100$ ) under the influence of a weak El Niño event (See Supplementary Dataset S1).

Samplings were conducted over 2–3 days. The specific velocity of the water flow through the system is unknown. However, to decrease the large pressure gradient from the headwaters to urban area, several storage tanks located in the middle and upper parts of the distribution system (Figure 1) play an important role to control this issue. The latter also guarantees a more homogenous water residence time in the system, and thus, the high spatial resolution sampling campaigns conducted most likely targeted the same water. Samples within the aqueduct features were collected at available outlets or valves. Tap waters were collected in residential areas using the following protocol: taps were opened for at least 5 min to avoid stagnant water within the nearby pipe. Tap water was collected the same day in all samplings. All samples were collected and stored at 5 °C until analysis in 50 mL high-density polyethylene (HDPE) bottles with plastic inserts to avoid potential fractionation. Endmembers such as springs, surface waters, and wells were collected directly at the source, avoiding any potential interference within the structure of the aqueduct such as pipelines, transfer lines, storage tanks, among others. Overall, sample distribution corresponded to tap water (46.7 %), wells (21 %), storage units or tanks (13.0 %), springs (8.6 %), transfer lines/pumping units (6.7 %), and surface waters (4.1 %) (See Supplementary Figure S1).



### 3.2. Rainfall, spring, and surface water time series

Daily and weekly isotope measurements in rainfall (at the urban area of Heredia and the headwaters; Figure 1) ( $N = 704$ ) were combined with weekly spring ( $N = 96$ ) and surface water samples ( $N = 94$ ) during 2018 and 2019 to complement the analysis of water source origin within the aqueduct. Rainfall was collected in passive devices (Palmex Ltd., Croatia) [29], while grab samples were collected at the spring and stream (See Supplementary Dataset S1). All samples were filtered using a Midisart polytetrafluorethylene (PTFE) 0.45  $\mu\text{m}$  syringe membrane (Sartorius AG, Germany), transferred to 30 mL HDPE bottles, and stored at 5 °C until analysis. Long-term stream and spring samples are included in the analysis with the aim to provide robust statistics of representative water sources at the headwaters and to analyze the predominance of rainfall generation across the west–east high elevation boundary. Previous studies have recognized complex rainfall generation systems at the continental divide, which are ultimately reflected in a clear isotope separation [19–21].

### 3.3. Stable isotopes analysis

Stable isotope analysis was conducted at the Stable Isotope Research Group facilities of the Universidad Nacional of Costa Rica using a water isotope analyzer LWIA-45P (Los Gatos Research Inc., USA). The secondary standards were MTW ( $\delta^2\text{H} = -131.4$  ‰,  $\delta^{18}\text{O} = -17.0$  ‰), DOW ( $\delta^2\text{H} = -1.7$  ‰,  $\delta^{18}\text{O} = -0.2$  ‰), and CAS ( $\delta^2\text{H} = -64.3$  ‰,  $\delta^{18}\text{O} = -8.3$  ‰). MTW and DOW standards were used to normalize the results to the VSMOW-SLAP scale, while CAS was used as a quality control and drift control standard. The analytical long-term uncertainty was:  $\pm 0.5$  (‰) ( $1\sigma$ ) for  $\delta^2\text{H}$  and  $\pm 0.1$  (‰) ( $1\sigma$ ) for  $\delta^{18}\text{O}$ . Isotopic compositions are presented in delta notation  $\delta$  (‰, per mil), relating the ratios ( $R$ ) of  $^{18}\text{O}/^{16}\text{O}$  and  $^2\text{H}/^1\text{H}$ , relative to Vienna Standard Mean Ocean Water (V-SMOW). Deuterium excess was calculated as  $d\text{-excess} = \delta^2\text{H} - 8 \delta^{18}\text{O}$  [30].

### 3.4. Stable isotope Bayesian mixing model

We adapted the stable isotope mixing model from the R package *Simmr* [31] to partition relative source water contributions for each aqueduct sampling using a Bayesian statistical framework based on a Gaussian likelihood. Five endmembers were selected: headwater rainfall (west), headwater rainfall (east), wells, springs, and surface water sources. Similarly, in an attempt to understand headwater hydrological functioning, relative contributions of two rainfall endmembers (west and east) to a spring and stream were also determined.

The main advantage of Bayesian mixing models over simple linear models relies on the ability to input isotope data from multiple sources [32–34]. Simple linear mixing models are not appropriate when putative sources are greater than the number of isotope tracers  $n$  plus one ( $n+1$ ) [35]. For instance, this model has been used to determine the contribution of (a) different soil depths in plant water use in a salt marsh flooding gradient [36] and summer maize [33]; and (b) groundwater and surface water sources to transpiration [32]. A Kruskal–Wallis non-parametric [37] one-way analysis of variance on ranks was conducted to diagnose significant differences among the endmembers. In addition, for all groups having a significant difference, an all pairwise multiple comparison procedure

was applied using Dunn's method [38] to test if there is evidence of stochastic dominance between the groups. The differences in the median values among the groups are greater than would be expected by chance; thus, there is a statistically significant difference ( $p < 0.001$ ). Similar to [32], trophic enrichment factors and concentration dependence values were set to zero as part of the model adaptation.

The model requires three sets of input data as a minimum to determine the proportions of water used within the aqueduct. We included: (i)  $\delta^2\text{H}$  and  $\delta^{18}\text{O}$  of the aqueduct (known as the mixture; three sampling campaigns), (ii) mean  $\delta^2\text{H}$  and  $\delta^{18}\text{O}$  for the endmembers and (iii) standard deviations of  $\delta^2\text{H}$  and  $\delta^{18}\text{O}$  for the endmembers [31]. *Simmr* was implemented with 100,000 iterations discarding the first 10,000. No prior information was used resulting in an equal likelihood of all sources [32]. The estimated source water contributions to the aqueduct mixture were determined using a Markov Chain Monte Carlo (MCMC) function [39] to repeatedly estimate the proportions of the various sources in the mixture and determine the values which best fit the mixture data [31]. Gelman–Rubin diagnostic [40] was performed to test model convergence using  $\delta^2\text{H}$  and  $\delta^{18}\text{O}$  values. The Gelman–Rubin diagnostic evaluates MCMC convergence by analyzing the difference between multiple Markov chains. Overall, all selected runs exhibited good model convergences (Gelman–Rubin value equals 1). Median (50 % quantile) source water contribution from the posterior parameter distribution was used for practical comparisons of the aqueduct operation in Figures 6 and 7. Supplementary Table S1 includes median and standard deviation values for all endmembers: rainfall (west and east), springs, wells, and surface waters.

## 4. Results

### 4.1. Sources and aqueduct isotope variability

In the study area, long-term mean annual rainfall exhibited a strong orographic difference between the urban area (city of Heredia;  $\sim 1168$  m asl) and the headwaters (Barva volcano edifice;  $\sim 1500$ – $2906$  m asl) (Figure 2, lower panel). The relationship of  $\delta^2\text{H}$  and  $\delta^{18}\text{O}$  values in rainfall (urban and headwaters), spring, stream, and the aqueduct is presented in Figure 3 along with the Global Meteoric Water Line (GMWL) and the Costa Rica MWL as references [41,42]. In general, all sources evidenced a clear and strong meteoric origin. To the west of the headwaters, rainfall  $\delta^{18}\text{O}$  and  $\delta^2\text{H}$  ranged from  $-20.2$  to  $-0.5$  ‰ (mean =  $-7.7$  ‰) and from  $-137.4$  to  $+7.2$  ‰ (mean =  $-48.9$  ‰), respectively. To the east,  $\delta^{18}\text{O}$  and  $\delta^2\text{H}$  ranged from  $-20.1$  to  $+0.4$  ‰ (mean =  $-5.2$  ‰) and from  $-156.5$  to  $-14.3$  ‰ (mean =  $-29.9$  ‰), respectively. Deuterium excess at both sites reflected significant moisture recycling processes, with mean  $d$ -excess values above  $+12$  ‰. In the urban area, rainfall isotope values presented a normal distribution with a mean of  $-7.3$  and  $-49.0$  ‰ (Figure 2(A–B)) for  $\delta^{18}\text{O}$  and  $\delta^2\text{H}$ , respectively. Details related to distinct rainfall generation mechanisms in this region were presented in previous studies [18–22,28,41].

The long-term spring site (near Sacramento, Figure 1), located at the west end of the study area, exhibited a left-skewed distribution with  $\delta^{18}\text{O}$  and  $\delta^2\text{H}$  values ranging from  $-10.0$  to  $-7.8$  ‰ (mean =  $-8.6$  ‰) and from  $-60.8$  to  $-48.5$  ‰ (mean =  $-53.8$  ‰), respectively. In contrast, the long-term stream site (red star symbol in Figure 1), located in the Caribbean slope of the headwaters, presented a right-skewed distribution with  $\delta^{18}\text{O}$

and  $\delta^2\text{H}$  values ranging from  $-9.9$  to  $-3.1$  ‰ (mean =  $-5.9$  ‰) and from  $-71.1$  to  $-8.5$  ‰ (mean =  $-32.6$  ‰), respectively. Similarly,  $d$ -excess at both sites averaged  $+14.0$  ‰ (Figure 2(A–B)).

Aqueduct samples were distributed between  $-9.9$  and  $-2.3$  ‰ for  $\delta^{18}\text{O}$  and  $-60.3$  and  $-6.8$  ‰ for  $\delta^2\text{H}$ . Similarly,  $d$ -excess ranged from  $+21.5$  to  $+7.7$  ‰. Lower  $d$ -excess values, particularly during the dry season, indicated evaporation across the aqueduct. Within the aqueduct the larger variability was reported in storage units or tanks, pumping units/transfer lines, and surface waters. Generally, groundwater and springs samples presented more constant isotopic compositions as a result of watershed damping effects and longer travel times and mixing.

#### 4.2. Temporal isotope patterns

Figure 3(C) shows temporal isotope variations during 2018 and 2019. In general, rainfall seasonality from dry (Jan–Apr) to wet season (May–Dec) was characterized by a W-shaped isotope pattern [22,43]. The latter is consistent with the pronounced intra-seasonal rainfall variations that results in isotopically two depleted (low  $\delta^{18}\text{O}$  values) incursions during the wet season and enriched pulses (high  $\delta^{18}\text{O}$  values) during July–August and December–March [22,44]. Both urban and headwater rainfall showed a similar pattern but different rainfall amounts (Figure 3(D–F)), affected by orographic (i.e. preferential condensation and removal of isotopically heavier molecules during water vapor uplift) and moisture transport processes across the continental divide (i.e. different air mass trajectories from the Caribbean or Pacific domains). In Central America, moisture transport often acts as an ‘atmospheric bridge’ that connects the semi-closed Caribbean Sea basin and the eastern Pacific warm pool. Stream isotopic composition clearly depicted rainfall isotope variations but mixing with previous isotopic conditions resulted in a relative attenuation of the isotope response. Spring  $\delta^{18}\text{O}$  values revealed a near-uniform composition around  $-8.6$  ‰, whereby longer groundwater flowpaths resulted in a stronger damping ratio than the stream system [44] (Figure 3(C)). Aqueduct isotopic compositions in September 2018 and 2019 (wet season peak) depicted the amplitude of the representative headwater sources (spring and stream). However, during the dry season sampling (April 2019), the aqueduct isotope amplitude was greater than the sources, evidencing strong secondary evaporation mainly across open storage tanks.

#### 4.3. Spatial trends

$\delta^{18}\text{O}$  spatial patterns across the aqueduct are presented in Figure 4. During the wet seasons, high isotope spatial variability suggested a less controlled allocation when water is abundant in surface and spring sources. In the dry season, and under the influence of large water deficits such as in April 2019 (weak El Niño) [45], high  $\delta^{18}\text{O}$  values were reported towards the northeast portion of the aqueduct; however, more homogenous compositions were measured in the middle and lower areas due the large predominance of deep groundwater sources. In general, the western and northwestern regions of the pipeline network exhibited lower  $\delta^{18}\text{O}$  values than the eastern and north-eastern sections. This surface trend is also evident in the underlying groundwater isoscape [21] in Figure 4.

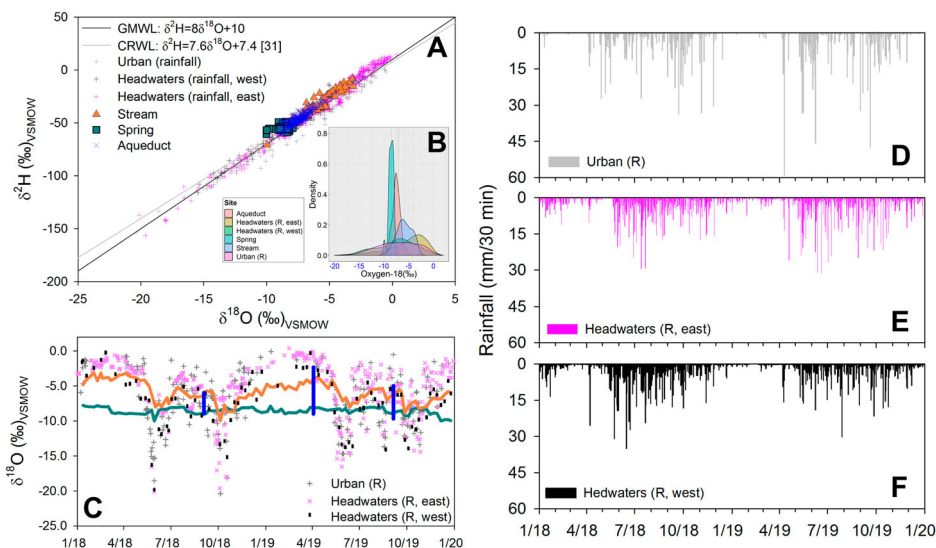


**Figure 3.** (A) Dual isotope diagram including rainfall (*R*; three sites), stream (triangles), spring (squares), and aqueduct (thin crosses) (See location in Figure 1). The Global Meteoric Water Line (GMWL) [41] and Costa Rican Meteoric Water Line (CRMWL) [42] are included as references. (B) Inset shows a density distribution plot for all sources. Dash lines denote median values per source. (C) Temporal isotope variations per source. Bold lines represent stream, spring, and aqueduct (vertical lines) time series. (D–F) Rainfall (mm/30 min) at the urban and headwater locations.

#### 4.4. Water source contributions

To highlight the importance of rainfall dynamics at the headwater region as part of an active component of a tropical urban system, water source contributions were first determined in two representative high elevation sources fed by east and west rainfall inputs (endmembers). Figure 5 shows dual isotope and density plots for both sources. Bayesian mixing results suggested a clear dominance of west rainfall with a median value of  $68.7 \pm 3.4\%$  within the spring discharge. In the stream, east rainfall contributed only  $55.8 \pm 3.9\%$ . Moisture transport from the Pacific slope provided large rainfall inputs in September and October within the northeastern sources, reflected in a mean value of  $44.2 \pm 3.9\%$ .

In the aqueduct, five endmembers were used: prior rainfall (east and west), wells, springs, and surface water (Figures 6–8). In September 2018 (wet season), the most dominant isotopic compositions were linked to surface water ( $44.2 \pm 3.9\%$ ) and springs ( $34.9 \pm 9.8\%$ ). Enough water surplus (water transported by gravity) decreased the use of groundwater pumping to only  $13.2 \pm 3.9\%$ , whereas new water (recent rainfall) accounts only for a total of  $7.9\%$ . Rainfall deficit due to a weak El Niño [45] event changed water contributions in 2019. For example, in the dry season groundwater pumping predominated with a  $37.5 \pm 22.1\%$  followed by spring supply ( $31.9 \pm 24.5\%$ ), with a small surface water contribution ( $7.7 \pm 5.1\%$ ). Cold front rainfall generated between December and February contributed  $20\%$ . Interestingly, the propagation of the rainfall deficit during the wet season forced a continuous use of deep groundwater sources ( $39.4 \pm 16.4\%$ ) followed by spring supply ( $29.5 \pm 19.4\%$ ) in September 2019. Surface water and direct rainfall

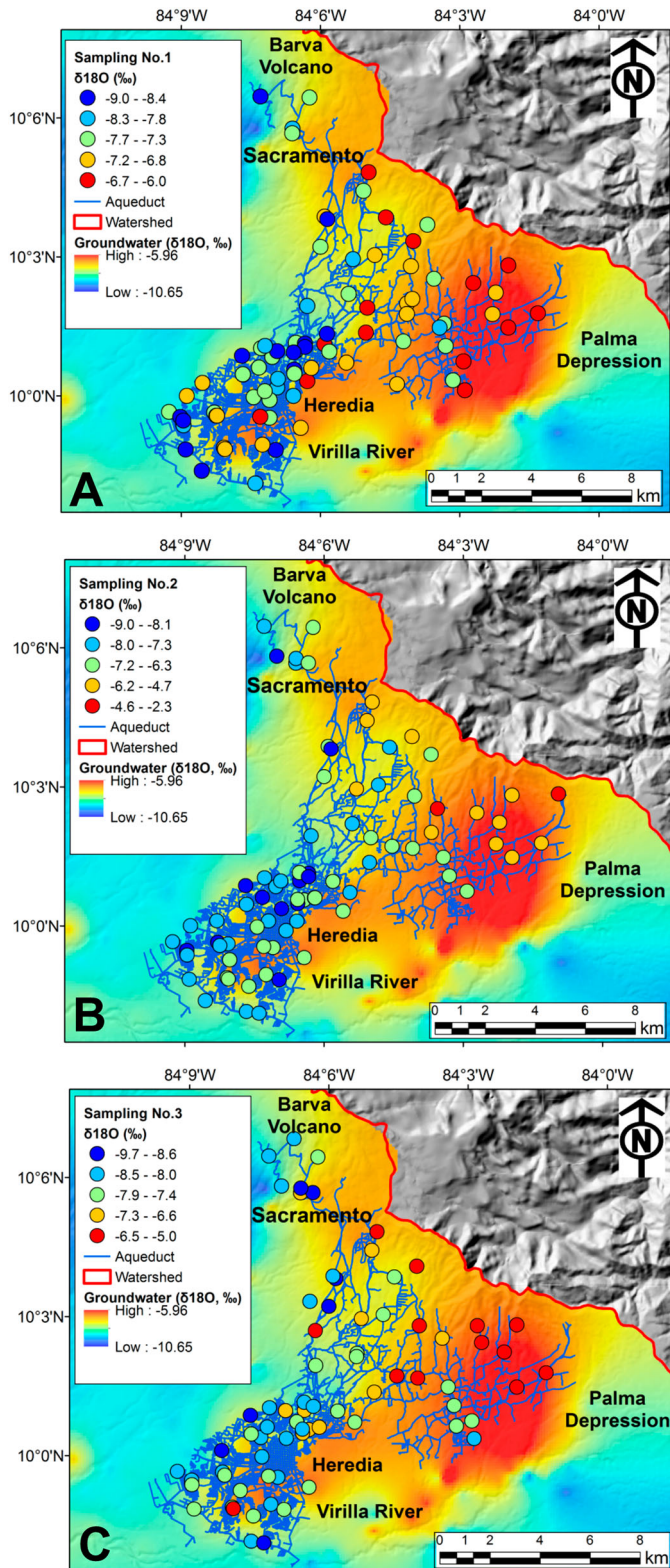


**Figure 4.** Distribution of  $\delta^{18}\text{O}$  (‰) across the aqueduct during (A) September 2018 (wet season); (B) April 2019 (dry season), and (C) September 2019 (wet season). A background groundwater isoscape [19] and pipeline network are presented as references.



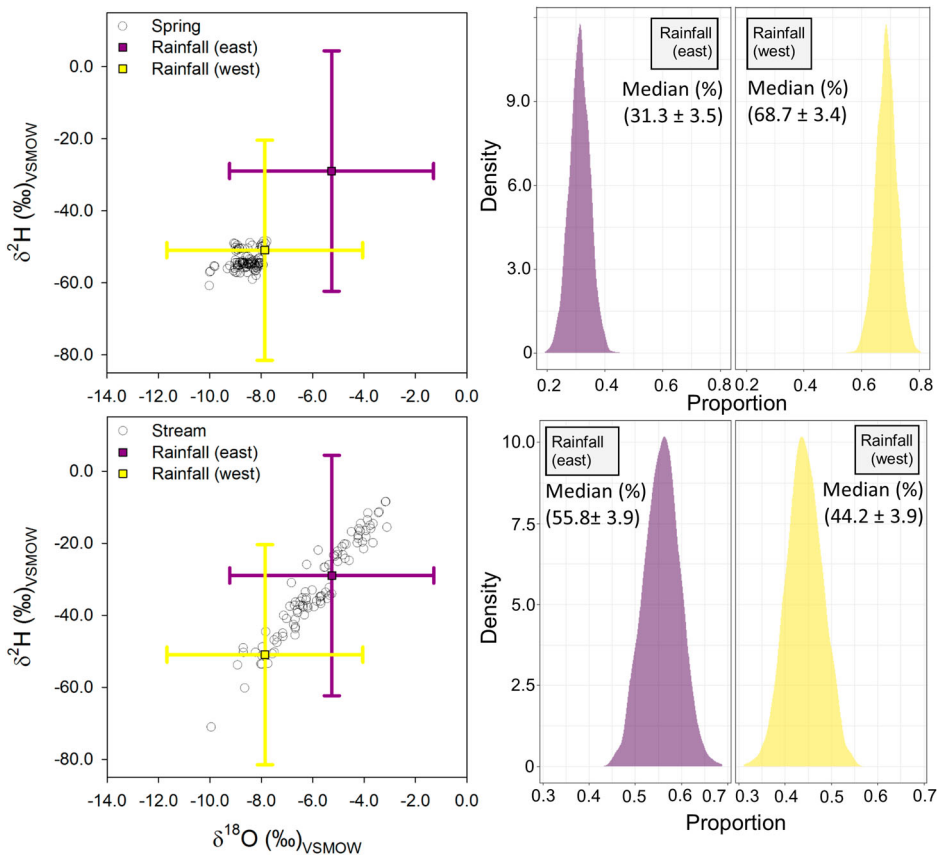


**Figure 5.** Left panel shows dual isotope diagrams for both mixtures (spring and stream; empty circles) and mean values of two endmembers (rainfall east and west). Right panel shows density plots relative to the proportion of each endmember.

contributed 10.5 and 15.8 %, respectively. Groundwater extraction was concentrated within the BCS (Figure 2, upper panel).

## 5. Discussion

Understanding the vulnerability of freshwater sources is crucial for water managers to improve water security and sustainability under recurrent climatic and anthropogenic pressures. Water isotopes have become a well-established and reliable tool in many fields of hydrology, as isotopes can provide important information to water managers for assessing sources and interactions. In the tropics water stable isotopes have been widely used to underpin hydrogeological and atmospheric processes [46,47], but their application in urban environments is still quite limited.

The provision of water for domestic supply in the Central Valley of Costa Rica [6] is indeed complex and usually involves many sources (i.e. deep and shallow groundwater, surface water, and spring water), and water reuse is minimal. Overall, tap water disproportionately depends on high elevation recharge in 'mountain water towers' and is

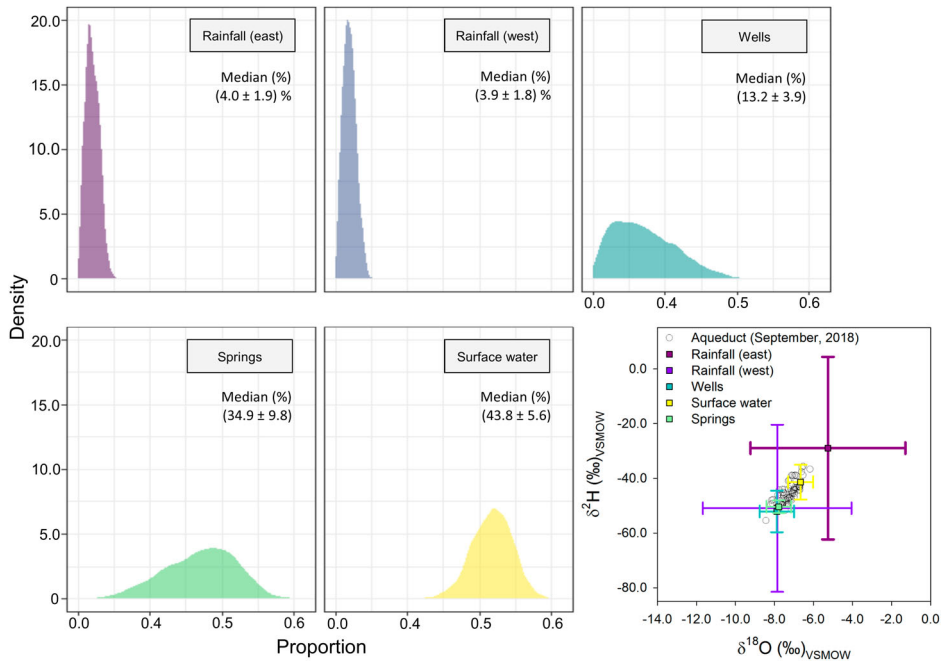


**Figure 6.** Density plots relative to the proportion of each endmember across the aqueduct during September 2018 and dual isotope diagram for aqueduct mixture (empty circles) and mean values of five endmembers. Median contributions of each endmember and uncertainties are also reported.

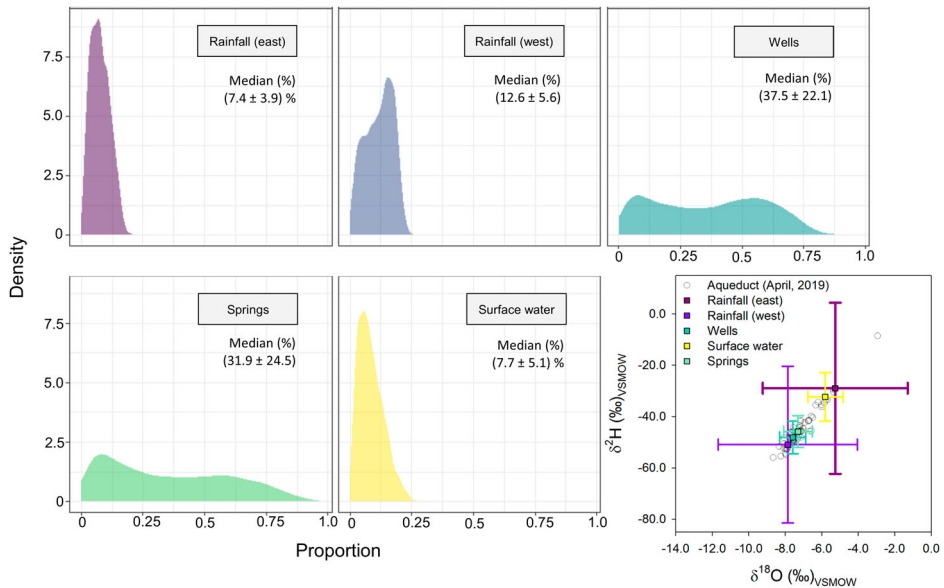


**Figure 7.** Density plots relative to the proportion of each endmember across the aqueduct during April 2019 and dual isotope diagram for aqueduct mixture (empty circles) and mean values of five endmembers. Median contributions of each endmember and uncertainties are also reported.



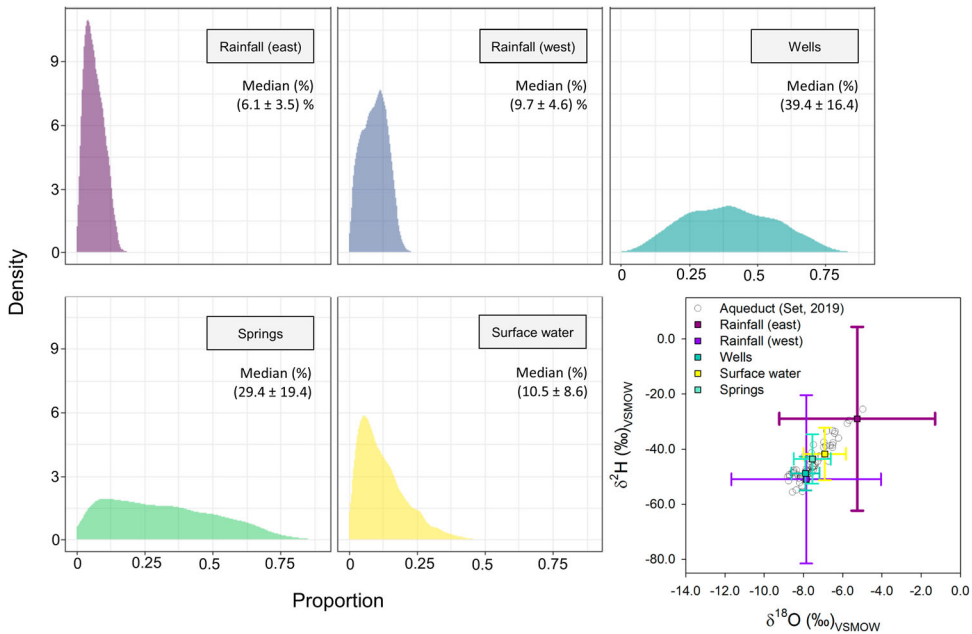


**Figure 8.** Density plots relative to the proportion of each endmember across the aqueduct during September 2019 and dual isotope diagram for aqueduct mixture (empty circles) and mean values of five endmembers. Median contributions of each endmember and uncertainties are also reported.

disproportionately supplied to lowland urban settlements [16,48], which in turns increases social pressure over water operators during rainfall deficit periods. Therefore a better ability to distinguish and map complex aqueduct interactions and sources may be useful for future planning and conservation practices in critical recharge areas [9].

To our knowledge and based on published literature, our results are the first aqueduct isoscape in a humid tropical region. Results suggested a strong spatial clustering within the aqueduct, indicating that nearby sites are characterized by similar drinking water isotope values and seasonal patterns. Two representative high elevation water sources (spring and stream) exhibited strong connections with rainfall isotope orographic and transport separations. Propagation of distinct isotopic pulses was traced from the headwaters to the cities. Low  $\delta^{18}\text{O}$  values were consistently clustered in the northwestern and lowland regions, whereas high  $\delta^{18}\text{O}$  values were grouped in the northeastern and southeastern regions.

Remarkably, during the wet season of 2018, stable isotopes revealed a less organized aqueduct structure with high  $\delta^{18}\text{O}$  values in the middle and lower urban areas. The latter can be explained by the rationale of more flexible hydraulic practices during water excess periods. In contrast, during the dry season (2019), accumulated rainfall deficit forced water operators to constrain water movement and allocation (recurrent water shortages on daily basis), resulting in more homogenous isotope values across most of the aqueduct, since groundwater prevailed as the main source. Spring and surface water source contributions were more important in normal operations under water excess timeframes. In fact, seasonal  $\delta^{18}\text{O}$  amplitude (1.19 ‰) was greater during the dry season (April 2019). Amplitudes during both wet seasons were significant lower

0.67 ‰ (September 2018) and 0.87 ‰ (September 2019), indicating a rather rapid water movement between storage units and pipelines, and less potential evaporative losses in the system.

The large dependency on groundwater extraction from the BCS (Figure 2; lower panel) during water stress periods, mainly due to the inter-annual rainfall variability in the region, is posing a conundrum for water resources management and drinking water allocation. This study, based on high resolution spatial isotope snapshots and community science involvement, was able to (a) describe multiple municipal sources, (b) identify water allocation in a tropical aqueduct during contrasting wet and dry conditions, (c) provide groundwater versus surface water mixing ratios, and (d) evaluate aqueduct management practices in the light of climatic and anthropogenic forcing. Similarly, our study is a novel and valid example for other tropical developing regions, whereby effective water allocation strategies may depend on a better knowledge of the aqueduct functioning.

## 6. Conclusions

Our study presents a novel and pioneer spatiotemporal analysis of headwater rainfall generation and the propagation of distinct isotopic pulses throughout a tropical urban drinking water distribution system during contrasting wet and dry seasons. We demonstrated that during water excess periods (2018), isotope values were more variable and randomly distributed, suggesting less oriented water allocation by the drinking water operator. Interestingly, the aqueduct management during 2019 was similar in both dry and wet seasons with a large predominance of groundwater extraction, which in turn demonstrates that climatic conditions are already posing a high social pressure on intra-seasonal decision making by drinking water operators. Isotope enrichment within the northeastern section of the aqueduct revealed a potential water storage deficiency and longer residence times that facilitate evaporation losses, particularly in storage tanks.

Water source contributions obtained from a Bayesian statistical framework highlight the potential of stable isotopes as a reliable tool to trace water engineering practices across a complex pipeline network. Future work should include (a) high resolution sampling in tap water (hourly sampling over 1–2 days) and key aqueduct features; (b) determination of net water losses across the aqueduct (leakage or evaporative losses); and (c) estimation of potential urban recharge versus headwater recharge. This information provides a rather low cost and feasible tool to map aqueduct water sources and allocations in order to assess water urban resilience to face an increasing residential and commercial water demand under different global warming scenarios.

## Acknowledgements

The authors thank the numerous university colleagues for helping with coordinated tap water sampling.

## Disclosure statement

No potential conflict of interest was reported by the author(s).

## Funding

This study was supported by International Atomic Energy Agency research contract No. 22760 to RSM as part of the Coordinated Research Project F33024 entitled 'Isotope Techniques for the Evaluation of Water Sources for Domestic Supply in Urban Areas'. A Joint Research Agreement between Universidad Nacional (Heredia, Costa Rica) and Empresa de Servicios Públicos de Heredia (ESPH S.A.) was also fundamental. Funding from the Research Office of Universidad Nacional through grant SIA [0332-18] to RSM entitled 'From Mountains to Cities: mapping multiple water sources and distribution in the Central Valley of Costa Rica' was crucial for conducting sampling campaigns and isotopic analysis.

## ORCID

Lucia Ortega  <http://orcid.org/0000-0002-5181-9054>

## References

- [1] United Nations. Global sustainable development report, 2015 edition. [Internet]. Available from: <https://www.un.org/en/development/desa/publications/global-sustainable-development-report-2015-edition.html>
- [2] Mbava N, Mutema M, Zengeni R, et al. Factors affecting crop water use efficiency: a worldwide meta-analysis. *Agr Water Manage.* 2020;228:105878.
- [3] Aznar-Sánchez JA, Belmonte-Ureña LJ, Velasco-Muñoz JF, et al. Economic analysis of sustainable water use: a review of worldwide research. *J Clean Prod.* 2018;198:1120–1132.
- [4] Gurdak JJ. Groundwater: climate-induced pumping. *Nat Geosci.* 2017;10(2):71–71.
- [5] Famiglietti JS. The global groundwater crisis. *Nat Clim Change.* 2014;4(11):945–948.
- [6] Bower KM. Water supply and sanitation of Costa Rica. *Environ Earth Sci.* 2014;71(1):107–123.
- [7] Esquivel-Hernández G, Sánchez-Murillo R, Birkel C, et al. Climate and water conflicts coevolution from tropical development and hydro-climatic perspectives: a case study of Costa Rica. *J Am Water Resour Assoc.* 2018;54(2):451–470.
- [8] Ehleringer JR, Barnette JE, Jameel Y, et al. Urban water – a new frontier in isotope hydrology. *Isot Environ Health Stud.* 2016;52(4–5):477–486.
- [9] Jameel Y, Brewer S, Good SP, et al. Tap water isotope ratios reflect urban water system structure and dynamics across a semiarid metropolitan area. *Water Resour Res.* 2016;52:5891–5910.
- [10] Grimmeisen F, Lehmann MF, Liesch T, et al. Isotopic constraints on water source mixing, network leakage and contamination in an urban groundwater system. *Sci Total Environ.* 2017;583:202–213.
- [11] Bonneau J, Fletcher TD, Costelloe JF, et al. Stormwater infiltration and the 'urban karst' – a review. *J Hydrol.* 2017;552:141–150.
- [12] Tipple BJ, Jameel Y, Chau TH, et al. Stable hydrogen and oxygen isotopes of tap water reveal structure of the San Francisco Bay area's water system and adjustments during a major drought. *Water Res.* 2017;119:212–224.
- [13] Jameel Y, Brewer S, Fiorella RP, et al. Isotopic reconnaissance of urban water supply system dynamics. *Hydrol Earth Syst Sci.* 2018;22(11):6109–6125.
- [14] Tian C, Wang L, Tian F, et al. Spatial and temporal variations of tap water <sup>17</sup>O-excess in China. *Geochim Cosmochim Acta.* 2019;260:1–14.
- [15] Deines JM, Liu X, Liu J. Telecoupling in urban water systems: an examination of Beijing's imported water supply. *Water Int.* 2016;41(2):251–270.
- [16] Yamanaka T, Yamada Y. Regional assessment of recharge elevation of tap water sources using the isoscape approach. *Mt Res Dev.* 2017;37(2):198–205.
- [17] Huang B, L'Heureux M, Hu ZZ, et al. Ranking the strongest ENSO events while incorporating SST uncertainty. *Geophys Res Lett.* 2016;43(17):9165–9172.

- [18] Sánchez-Murillo R, Durán-Quesada AM, Birkel C, et al. Tropical precipitation anomalies and *d*-excess evolution during El Niño 2014–16. *Hydrol Process*. 2017;31(4):956–967.
- [19] Sánchez-Murillo R, Birkel C, Welsh K, et al. Key drivers controlling stable isotope variations in daily precipitation of Costa Rica: Caribbean Sea versus eastern Pacific Ocean moisture sources. *Quat Sci Rev*. 2016;131:250–261.
- [20] Sánchez-Murillo R, Esquivel-Hernández G, Sáenz-Rosales O. Isotopic composition in precipitation and groundwater in the northern mountainous region of the Central Valley of Costa Rica. *Isot Environ Health Stud*. 2017;53(1):1–17.
- [21] Sánchez-Murillo R, Birkel C. Groundwater recharge mechanisms inferred from isoscapes in a complex tropical mountainous region. *Geophys Res Lett*. 2016;43(10):5060–5069.
- [22] Sánchez-Murillo R, Durán-Quesada AM, Esquivel-Hernández G, et al. Deciphering key processes controlling rainfall isotopic variability during extreme tropical cyclones. *Nat Commun*. 2019;10(1):4321.
- [23] Protti-Quesada R. Geología del flanco sur del Volcán Barva: Heredia, Costa Rica. *Boletín de Vulcanología*. 1986;17:23–31.
- [24] BGS/SENARA. The continuation of hydrogeological investigations in the north and east of the Valle Central, Costa Rica. Final report 1984–1987. British Geological Survey Technical report WD/88/13R. San José, 1988.
- [25] Espinoza A, Morera A, Mora D, et al. Drinking water quality in Costa Rica: current situation and prospects (San José, Costa Rica). Ministerio de Salud – Instituto Costarricense de Acueductos y Alcantarillados – Organización Panamericana de la Salud Organización Mundial de la Salud. Available from: [https://www.paho.org/cor/index.php?option=com\\_content&view=article&id=143:publicaciones&Itemid=221](https://www.paho.org/cor/index.php?option=com_content&view=article&id=143:publicaciones&Itemid=221)
- [26] Waylen PR, Caviedes CN, Quesada ME. Interannual variability of monthly precipitation in Costa Rica. *J Clim*. 1996;9:2606–2613.
- [27] Salas-Navarro J, Sánchez-Murillo R, Esquivel-Hernández G, et al. Hydrogeological responses in tropical mountainous springs. *Isot Environ Health Stud*. 2018;55(1):25–40.
- [28] Arriagada RA, Sills EO, Ferraro PJ, et al. Do payments pay off? Evidence from participation in Costa Rica's PES program. *PLoS One*. 2015;10(8):e0136809.
- [29] Gröning M, Lutz HO, Roller-Lutz Z, et al. A simple rain collector preventing water re-evaporation dedicated for  $\delta^{18}\text{O}$  and  $\delta^2\text{H}$  analysis of cumulative precipitation samples. *J Hydrol*. 2012;448:195–200.
- [30] Dansgaard W. Stable isotopes in precipitation. *Tellus*. 1964;16:436–468.
- [31] Parnell A, Inger R. Stable isotope mixing models in R with *simmr*; 2016. Available from: <https://cran.r-project.org/web/packages/simmr/vignettes/simmr.html>
- [32] Gokool S, Riddell ES, Swemmer A, et al. Estimating groundwater contribution to transpiration using satellite-derived evapotranspiration estimates coupled with stable isotope analysis. *J Arid Environ*. 2018;152:45–54.
- [33] Ma Y, Song X. Using stable isotopes to determine seasonal variations in water uptake of summer maize under different fertilization treatments. *Sci Total Environ*. 2016;550:471–483.
- [34] Correa A, Ochoa-Tocachi D, Birkel C. Uncertainty in multi-source partitioning using large tracer data sets. *Hydrol Earth Syst Sci*. 2019;23(12):5059–5068.
- [35] Zhang ZQ, Evaristo J, Li Z, et al. Tritium analysis shows apple trees may be transpiring water several decades old. *Hydrol Process*. 2017;31:1196–1201.
- [36] Redelstein R, Coners H, Knohl A, et al. Water sources of plant uptake along a salt marsh flooding gradient. *Oecologia*. 2018;188(2):607–622.
- [37] Kruskal WH, Wallis WA. Use of ranks in one-criterion variance analysis. *J Am Stat Assoc*. 1952;47(260):583–621.
- [38] Dunn OJ. Multiple comparisons among means. *J Am Stat Assoc*. 1961;56(293):52–64.
- [39] Brooks S. Markov chain Monte Carlo method and its application. *J R Stat Soc D*. 1998;47(1):69–100.
- [40] Gelman A, Rubin DB. Inference from iterative simulation using multiple sequences. *Stat Sci*. 1992;7(4):457–472.
- [41] Craig H. Isotopic variations in meteoric waters. *Science*. 1961;133(3465):1702–1703.

- [42] Sánchez Murillo R, Esquivel Hernández G, Welsh K, et al. Spatial and temporal variation of stable isotopes in precipitation across Costa Rica: an analysis of historic GNIP records. *Open J Mod Hydrol.* [2013](#);3:226–240.
- [43] Sánchez-Murillo R, Esquivel-Hernández G, Corrales-Salazar J, et al. Tracer hydrology of the data-scarce and heterogeneous Central American Isthmus. *Hydrol Process.* [2020](#);34(11):2660–2675.
- [44] Sánchez-Murillo R, Romero-Esquivel LG, Jiménez-Antillón J, et al. DOC transport and export in a dynamic tropical catchment. *J Geophys Res Biogeosci.* [2019](#);124:1665–1679.
- [45] Johnson NC, L’Heureux ML, Chang CH, et al. On the delayed coupling between ocean and atmosphere in recent weak El Niño episodes. *Geophys Res Lett.* [2019](#);46(20):11416–11425.
- [46] Munksgaard NC, Kurita N, Sánchez-Murillo R, et al. Data descriptor: daily observations of stable isotope ratios of rainfall in the tropics. *Sci Rep.* [2019](#);9(1):14419.
- [47] Jasechko S. Global isotope hydrogeology – review. *Rev Geophys.* [2019](#);57(3):835–965.
- [48] Immerzeel WW, Lutz AF, Andrade M, et al. Importance and vulnerability of the world’s water towers. *Nature.* [2020](#);577(7790):364–369.